Interdisciplinary Research in Medical Sciences Specialty
ISSN: 3062-4401
2021, Volume 1, Issue 1, Page No: 46-61

Available online at: www.galaxypub.co/page/journals

Galaxy Publication

Thermal Pyrolysis of Plastic Medical Waste (Syringes and Saline Bottles): Product Yield, Fuel Properties, and Chemical Characterization

Pierre Dubois[1], Laurent Moreau[1], Antoine Lefèvre[1], Nicolas Bernard[1]*

[1]Department of Clinical Pharmacology, Faculty of Medicine, University of Lyon, Lyon, France.

***E-mail** ✉ nicolas.bernard@outlook.com

Received: 08 January 2021; **Revised:** 05 March 2021; **Accepted:** 08 March 2021

ABSTRACT

This work explores the feasibility of producing alternative fuel through the pyrolysis of syringe waste (SW) and saline bottle waste (SBW). Plastic-derived medical refuse poses serious environmental and public health risks when mishandled. Laboratory runs were performed in a batch-type fixed-bed reactor, varying temperatures from 0 to 600°C at 50°C increments. The influence of temperature on product formation was examined. Key attributes of pyrolytic oil from SW and SBW—including density, kinematic viscosity, pour point, boiling point, and cloud point—were assessed. The measured ranges were 726–758 kg/m³, 3.19–4.75 cSt, −12 to −16°C, 86–95°C, −2 to −5°C, and the GCV remained close to 42–44 MJ/kg. Char exhibited a GCV of about 42–43 MJ/kg. GC-MS and FT-IR outcomes indicated elevated levels of alcohols and organosilicon compounds in oils derived from SW and SBW, respectively. TGA-DTG profiles revealed that thermal decomposition of these oils occurred primarily between 50–280°C. With adequate post-treatment, both liquid and solid fractions can function as energy sources or chemical intermediates for numerous sectors. The findings also demonstrate similarities to low-grade liquid fuels and high-quality solid fuels. The surge in medical waste during and after COVID-19 has produced significant disposal challenges. Pyrolyzing syringes and saline bottle waste can help mitigate pollution while offering a supplementary energy route.

Keywords: Pyrolysis, Medical waste, GC-MS, FT-IR, TGA-DTG curve, Pyrolytic oil

How to Cite This Article: Dubois P, Moreau L, Lefèvre A, Bernard N. Thermal Pyrolysis of Plastic Medical Waste (Syringes and Saline Bottles): Product Yield, Fuel Properties, and Chemical Characterization. Interdiscip Res Med Sci Spec. 2021;1(1):46-61. https://doi.org/10.51847/AHDNCGeSqO

Introduction

The global shortage of fossil energy has motivated the search for new, sustainable fuel options. Effective waste handling and suitable policy frameworks are key components of sustainable progress [1]. Managing clinical waste has become a crucial issue worldwide [2]. Rapid growth in healthcare services has resulted in a higher volume of medical refuse in developing nations. When not properly controlled, these wastes impose risks on individuals, communities, and ecosystems. Worldwide, 75–90% of healthcare refuse is non-hazardous and originates from routine or administrative activities of medical facilities [3]. Information on waste composition and generation for selected regions is illustrated in **Figure 1** and **Table 1** [4, 5].

Numerous elements influence the healthcare waste generation rate (HCWGR) [6]. In many developing countries, HCW output is rising sharply due to better access to medical care [7]. Landfilling is an unsuitable choice for disposing of plastic medical materials because of their slow breakdown. Mechanical recycling is possible but comes with constraints [8]. Pyrolysis represents an efficient pathway for converting plastic-based refuse into liquid fuels [9], producing useful hydrocarbons usable as energy sources or as feedstocks for chemical manufacturing [10].

During the COVID-19 crisis, medical waste volumes increased dramatically. Higher biomedical waste output has strained handling systems, intensifying worries regarding the dangers of unsafe disposal. Poorly managed

infectious medical waste can significantly harm public health. Robust systems for safe and efficient handling are necessary to reduce these risks [11–17].

A survey in Khulna City Corporation (KCC) documented a healthcare waste generation of approximately 1.29 kg/bed/day [18]. A comparable investigation in Jashore municipality reported 1.59 kg/bed/day [19]. Another assessment in the Rajshahi City Corporation (RCC) recorded 1.54 kg/bed/day [20]. Altogether, these studies indicate that major Bangladeshi cities produce around 1.5 kg/bed/day of healthcare waste.

Limited scientific literature has explored fuel generation from thermally decomposing medical refuse. Fahim *et al*. assessed how syringe components, cotton-swab rods, medical gloves, mixed hospital waste, and their combined samples behave during decomposition, focusing on synergistic effects, reaction pathways, and gaseous emissions by using TG-MS, TG-FT-IR, TGA, and several kinetic modeling tools [21]. Weijie *et al*. analyzed masks, mask straps, and infusion tubing to verify their pyrolysis routes and material features with TGA, vibrational spectroscopy, TG-FT-IR, and py-GCMS [22]. Ziyi *et al*. examined syringe debris and medical bottle materials, mapping out decomposition tendencies, controlling factors, mechanistic stages, product formation, and reaction routes with Py-GC/MS and TG-FT-IR, while considering degradation intervals, conversion percentages, and heat-rate variations [23]. Vasile *et al*. processed disposable syringes through pyrolysis and evaluated the resulting materials through density tests, gas-chromatographic profiling, aniline point determination, refractive index assessment, and a variety of spectroscopic procedures [24]. Deng *et al*. measured thermogravimetric patterns and relevant kinetic parameters for typical medical waste fractions [25]. Zhu *et al*. documented decomposition behavior for selected medical wastes using TGA linked to FT-IR (TG-FT-IR) [26]. Bernardo *et al*. assessed chars obtained by co-pyrolyzing PP, PE, and PS plastics with pine residues and shredded tires, focusing on their physicochemical properties [27]. Dash *et al*. investigated syringe-waste thermolysis and its potential for generating hydrocarbon-rich fractions [28]. Ahmad *et al*. contrasted properties of oils derived from PP and HDPE pyrolysis with those of Diesel and Gasoline [29]. Pramanik *et al*. produced oil from waste polyethylene in a customized semi-batch setup and characterized it by API gravity, carbon-residue percentage, fire point, calorific content, flash point, and proximate values [30]. Som *et al*. examined the recovery of useful outputs from plastic medical wastes (PMW) via pyrolysis. Polypropylene and high-density polyethylene represent the dominant polymers in discarded syringes and saline containers [8].

Energy recovery is a major motivation for pyrolyzing waste streams because the resulting liquids, gases, and solids typically show strong fuel-like attributes. Pyrolytic oils and chars often qualify as industrial feedstocks due to their advantageous physical and chemical properties. Gas from slow pyrolysis generally exhibits a heating capacity of 10–15 MJ/m³ [31]. For gases produced from PP and PE, the heating range spans 42–50 MJ/kg [32]. Fuel suitability of pyrolytic oil is typically evaluated by analyzing density, viscosity, boiling characteristics, pour and cloud points, and flash temperature [33]. Oils obtained from mixed plastics tend to display around 40 MJ/kg of heating value [34]. Many pyrolytic oils from plastic waste include notable quantities of toluene, styrene, and ethylbenzene, which can serve as precursors in chemical manufacturing [35]. In comparison, oils from PET are less practical owing to their strong acidity [36]. Solid char from waste pyrolysis frequently carries a heating value close to 34 MJ/kg [37], which is similar to that of bituminous coal.

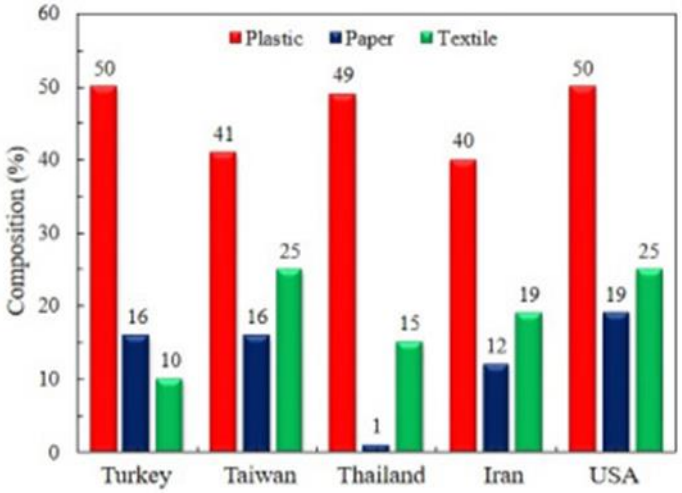

Figure 1. Medical waste composition of different countries

Table 1. Healthcare waste generation rates in selected countries

Country	HCWGR (kg/Bed/Day)	References
Bangladesh	1.24	[38, 39]
India	1.55	[40]
Pakistan	2.07	[41]
Nepal	0.5	[42]
Malaysia	1.9	[42]
Indonesia	0.75	[43]
Thailand	2.05	[44]
Iran	3.04	[42, 45]
France	3.3	[41]
United Kingdom	3.3	[41]
Germany	3.6	[46]
China	4.03	[47, 48]
Canada	8.2	[49]
United States of America	8.4	[41, 49, 50]

Materials and Methods

Raw materials

A range of tools, analytical items, and supporting materials was required to convert SW/SBW into pyrolytic gas, oil, and char. The discarded syringe units and saline bottles used in the study originated from clinics and hospitals in Khulna city, Bangladesh. These items were thoroughly rinsed with detergent and water to eliminate dirt, blood residues, and other deposits. Afterward, the cleaned materials were dried in sunlight and cut into smaller segments with scissors, as shown in **Figure 2**.

a) b)

Figure 2. Chopped SW and SBW

Characterization of raw materials

Proximate and ultimate analyses were completed using a muffle furnace (SX-7-10D, USA) at 950°C and a CHNS analyzer (varioMicro V1.6.1, GmbH, Germany). TGA measurements employed a TGA-50H system from Shimadzu, Japan. GC-MS work was carried out with a GCMS-TQ8040 unit. FT-IR spectra were produced using an IRTracer-100 device (Shimadzu, Japan). Gross calorific values of the feed materials were determined using an Oxygen Bomb Calorimeter from Infitek, USA.

Experimental setup and procedure

The primary reaction vessel was a stainless-steel cylinder measuring 27.0 cm in length. Its outer and inner diameters were 22.7 cm and 22.0 cm, respectively. A schematic of the arrangement is provided in **Figure 3**. One

side of the chamber was sealed, while the opposite side functioned as the feed inlet. To minimize thermal loss, the unit was insulated with asbestos rope. Internal temperatures were monitored using K-type thermocouples connected to a display interface.

An amount of 1 kg of chopped SW or SBW was first weighed, then loaded into the reactor by opening the upper lid. Heating was delivered by three uniformly spaced U-shaped electric elements mounted inside the system. Processing occurred in an oxygen-free environment; nitrogen was continuously supplied to keep the chamber inert. A heating rate of roughly 10°C/min was maintained. For each SW and SBW trial, the temperature was increased through the 0–600°C range, holding each temperature setting for 30 minutes. As the temperature rose, the feed material broke down into gaseous products, which then flowed through a connector tube to the condenser. Chilled water circulated via a pump over copper coils to liquefy the vapors.

Non-condensable gases were vented by flaring. Heating continued until gas evolution ceased. The condensed fraction collected below the condenser was gathered in a receiving container and subsequently filtered to divide wax from liquid oil. After the run, the heaters were switched off to allow cooling, and the remaining solids—mainly pyrolytic char with trace ash—were retrieved. The char was screened to remove coarse pieces and washed repeatedly with water to eliminate ash and soluble impurities.

To determine product yields, the reactor was opened once the experiment finished, and the char was removed and weighed. The summed mass of liquid oil and solid char was then compared against the starting material. Gas yield was obtained by subtracting the oil and char weights from the initial feed. The mass of gaseous products (Wg) was calculated using:

$$Wg = Wf - (Wc + Wo) \quad (1)$$

where Wf is the initial mass fed, Wc is the recovered char, and Wo is the collected oil [8].

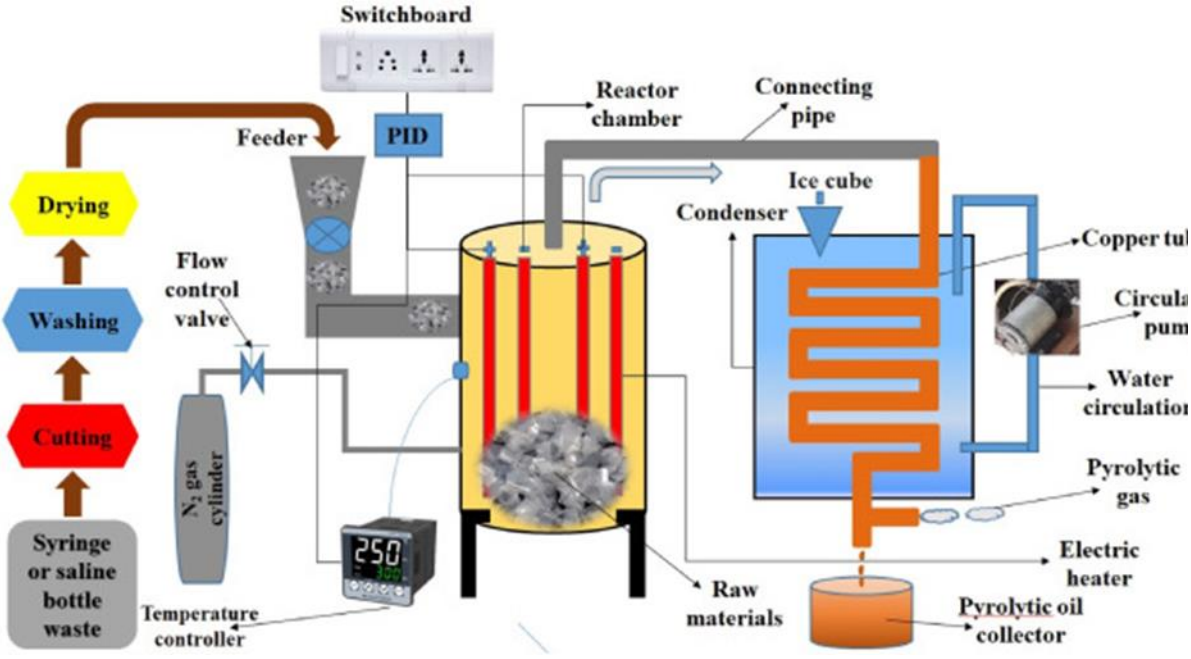

Figure 3. Schematic diagram of the experimental set-up

Characterization methods of pyrolytic oil

Density, kinematic viscosity, pour point, boiling point, and cloud point of oils derived from SW and SBW were measured following ASTM standards D4052, D445, D97, D1120, and D5773, respectively. These findings were compared with earlier reports on Diesel and gasoline properties.

Results and Discussion

Proximate and ultimate analysis of raw materials

Combustion behavior of fuel samples involves the fraction that volatilizes (volatile matter), the solid carbon residue that remains (fixed carbon), the portion of inorganic, nearly inert material (ash), and the total moisture content, which expresses the water mass relative to the original wet weight. These metrics are crucial for accurately evaluating the fuel characteristics of biomass-type materials. **Table 2** presents the proximate and elemental composition for SW and SBW.

From **Table 2**, SBW exhibits a higher fixed-carbon percentage than SW, while SW shows slightly elevated volatile matter. Moisture and ash levels are almost the same for both feedstocks. Elemental carbon and hydrogen are more abundant in SW, whereas nitrogen content is lower. Sulfur is higher in SBW, with no measurable sulfur in SW.

Table 2. Proximate and ultimate analysis of raw syringe and saline bottle waste.

Proximate Analysis (wt%, as received)	**Syringe Waste (SW)**	**Saline Bottle Waste (SBW)**
Fixed carbon	34.06	36.13
Volatile matter	61.78	60.56
Moisture content	1.25	0.97
Ash content	2.91	2.34
Ultimate Analysis (wt%, dry ash-free basis)	**Syringe Waste (SW)**	**Saline Bottle Waste (SBW)**
Carbon (C)	84.66	67.50
Hydrogen (H)	16.11	6.76
Nitrogen (N)	1.54	12.38
Sulfur (Sulfur (S)	0.00	10.47

Thermogravimetric analysis (TGA) and TGA-DTG curve

TGA allows assessment of a material's resistance to heat and its stepwise degradation under inert or oxidative atmospheres. The pyrolysis oils obtained from SW and SBW were subjected to TGA at a heating rate of 10 °C/min in an oxidizing setting. The corresponding TG and DTG profiles are presented in **Figures 4 and 5**.

For SW **(Figure 4)**, the mass loss begins sharply at roughly 50 °C and persists until close to 150 °C, a region typically associated with evaporation of moisture and light compounds. From 150–250 °C, the decline in mass continues at a steadier pace, likely reflecting decomposition of moderately volatile constituents. Beyond 250 °C, the mass decreases slowly up to 550 °C, indicating that nearly all volatiles have been released and minimal char remains. The pronounced drop near 150 °C implies that most degradation occurs in the lower temperature interval examined. These comparatively reduced degradation temperatures may stem from additives, plasticizers, and stabilizing agents present in the polymer matrix [51].

In the DTG plot, the dashed red trace indicates the rate of mass change. A distinct maximum appears at about 150 °C, matching the rapid TG decline, and another peak is observed near 250 °C, marking a secondary decomposition step. Above 250 °C, the weight-loss rate becomes insignificant, signifying the end of the major thermal reactions. When the temperature is increased at 10 °C/min from 50–150 °C, **Figure 5** displays a strong initial mass reduction for SBW due to water, low-boiling species, and N_2 sweeping. Between 150–250 °C, the mass gradually decreases as less volatile organics decompose. For SBW oil, 50% mass loss occurs at roughly 150 °C, and decomposition is essentially complete by 340 °C, with almost no char left. The DTG curve shows its dominant peak near 150 °C, consistent with the greatest degradation rate, while a minor peak near 250 °C marks an additional reaction phase. After 250 °C, the mass-loss rate falls to nearly zero.

Overall, pyrolysis oil from syringe waste undergoes thermal breakdown at lower temperatures compared with that from saline bottle waste, producing minimal residue and fragmenting mainly within the 50–280 °C region in oxidizing conditions.

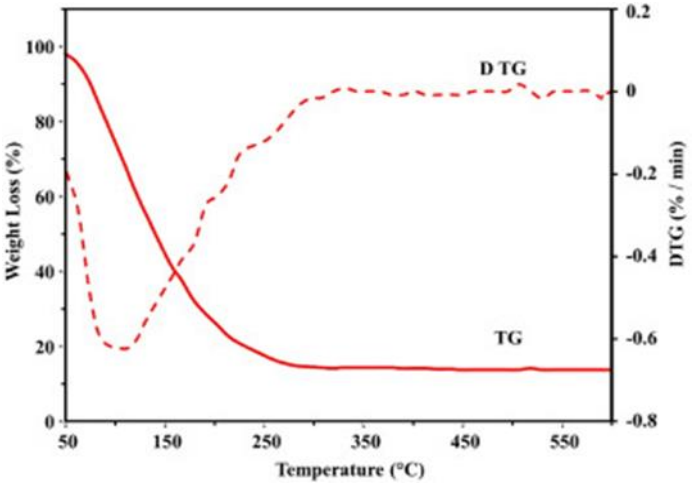

Figure 4. TGA-DTG curve of pyrolysis oil derived from SW

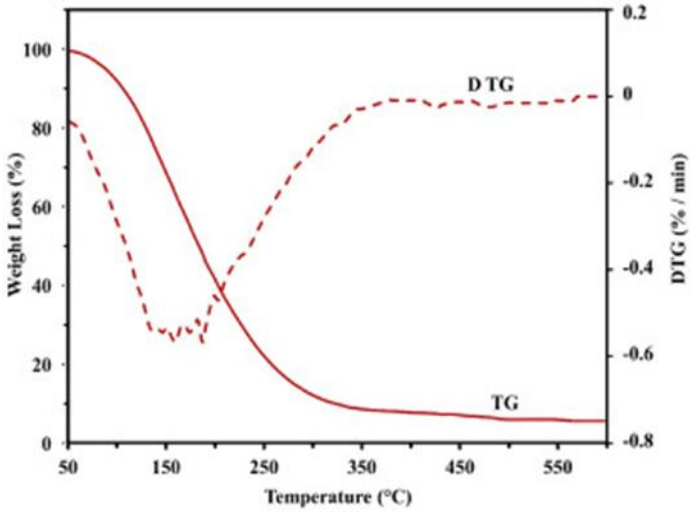

Figure 5. TGA-DTG curve of pyrolysis oil derived from SBW

Effect of temperature on product yield

Three experimental series were carried out, each covering twelve temperatures—50, 100, 150, 200, 250, 300, 350, 400, 450, 500, 550, and 600 °C—for both SW and SBW. Average values were used in evaluating temperature-dependent trends. The pyrolysis generated three product phases: liquid oil, solid char, and gaseous output. **Figures 6 and 7** summarize the yield variations for SW and SBW.

As illustrated in **Figures 6 and 7**, liquid production rises progressively with increasing temperature, reaching its maximum near 450 °C. In contrast, solid-phase yield declines as temperature increases. Gas formation stays relatively stable at lower temperatures but begins to rise noticeably once temperatures exceed 450 °C. Across the three repetitions, liquid yield consistently followed an upward pattern, peaking at 450 °C.

The highest oil yield (by mass) for SW was 53.2% at 450 °C, while its maximum char yield reached 73.1% at 50 °C. For SBW, the largest oil yield was 54.9% at 450 °C, and the greatest char production was 72.1% at 50 °C.

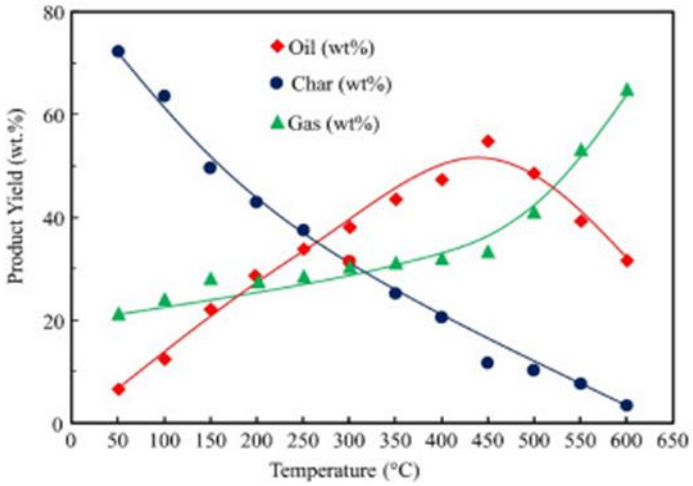

Figure 6. Temperature influence on product yield for SW

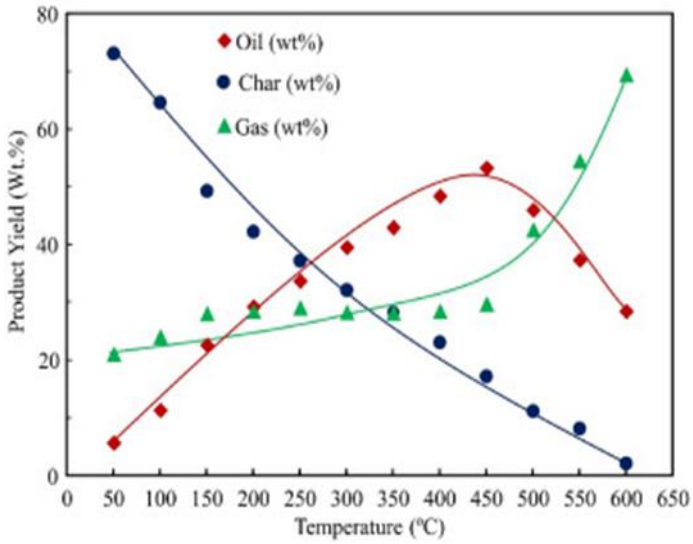

Figure 7. Temperature influence on product yield for SBW

Characterization of pyrolytic oil by GC–MS analysis

The primary products generated from SW and SBW were condensable liquids. Gas chromatography–mass spectrometry (GC–MS) was employed to identify and quantify constituents of the recovered oils. This technique was applied to characterize the molecular profile of the pyrolytic fractions and to explore potential routes for their handling and reuse [52]. The analyses were performed at the Bangladesh Council of Scientific and Industrial Research (BCSIR), Dhaka. **Figure 8**, **Table 3**, and **Figure 9** show the chromatogram, compound distribution, and comparative composition of the SW-derived oil produced at 450 °C.

According to **Table 3**, the pyrolysis oil contains notable amounts of compounds such as 1-decanol, 2-hexyl-, commonly used in formulations of surfactants, emulsifiers, lubricants, solvents, plasticizers, and fragrance additives; 11-methyldodecanol, applied in cosmetic, perfume, flavoring, and surfactant industries; and hexa-triacontyl-trifluoroacetate, utilized in coatings, protective films, and research activities. Similar findings have been reported in previous studies [8, 24, 28, 53, 54]. Various other detected molecules also have recognized industrial relevance.

Figure 9 presents the compositional comparison, indicating that SW pyrolytic oil contains alcohols as the most dominant class, while esters, alkenes, alkanes, and organosilicon compounds also appear.

For SBW-derived oil, **Figure 10**, **Table 4**, and **Figure 11** display the chromatogram, component distribution, and comparative analysis at 450 °C.

Table 4 shows that this oil contains higher levels of hexamethyl-cyclohexasiloxane (used in cosmetics, lubricants, and silicone polymer production), oxime-, methoxy-phenyl- (utilized in pharmaceuticals and synthetic chemistry), 6-methyl-2-phenylindole (applied in medicinal and organic synthesis research), 3,3-diisopropoxy-1,1,1,5,5,5-

hexamethyltrisiloxane (used in cosmetic and surface treatment formulations), perhydro-htx-2-one (used in fragrance and solvent applications), and 2-depentyl-, acetate ester (found in fragrance and solvent industries). Comparable compound types have been documented by other authors [8, 53, 54]. Additional molecules appearing in the analysis also hold industrial uses.

Figure 11 shows the compositional comparison for SBW, where organosilicons dominate the mixture. Aromatic compounds, esters, terpenes, and alcohols are also present.

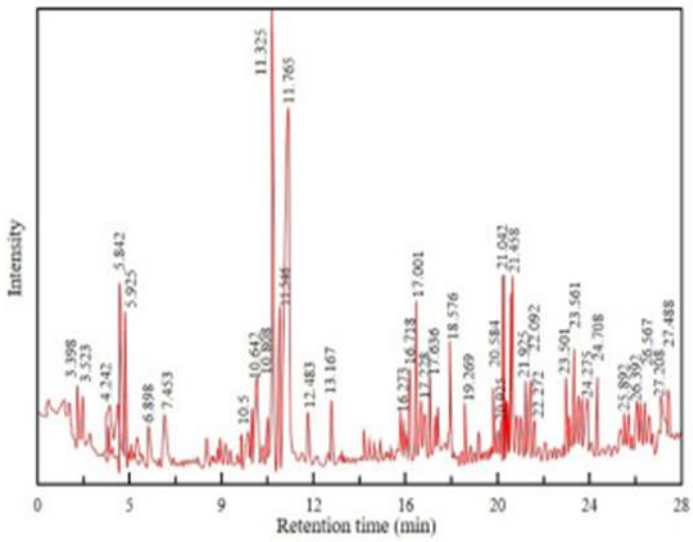

Figure 8. Chromatographic profile of pyrolytic oil from SW

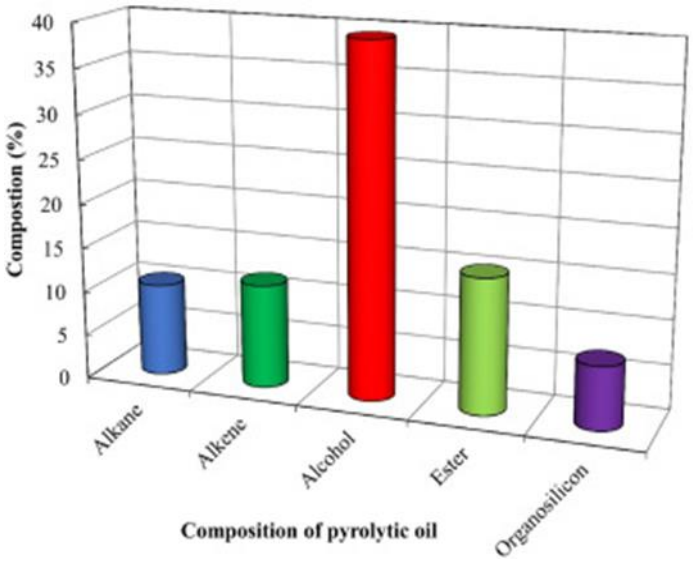

Figure 9. Compositional comparison of pyrolytic oil from SW

Table 3. Composition of pyrolytic oil from SW

Compound Class	Compound Name	Molecular Formula	Boiling Point (°C)	Peak Area (%)	Retention Time (min)
Alkanes	Dodecane, 4,6-dimethyl-	$C_{14}H_{30}$	235.5	1.06	10.642
	Decane, 1-iodo-	$C_{10}H_{21}I$	132	0.80	16.273
	Eicosane	$C_{20}H_{42}$	343	0.94	17.383
	Eicosane	$C_{20}H_{42}$	343	1.68	20.584
	Eicosane	$C_{20}H_{42}$	343	1.68	20.584
	1-Cyclopentyleicosane	$C_{25}H_{50}$	513	1.03	20.925

	1-Cyclopentyleicosane	$C_{25}H_{50}$	513	1.08	21.675
	Tetrapentacontane, 1,54-dibromo-	$C_{54}H_{108}Br_2$	830	0.81	26.392
	Tetrapentacontane	$C_{54}H_{110}$	596	1.65	23.501
	11-Methyltricosane	$C_{24}H_{50}$	–	1.31	23.991
Alkenes	2-Decene, 4-methyl-, (Z)-	$C_{11}H_{22}$	218	2.84	4.242
	2-Undecene, 4,5-dimethyl-, [R*,S*-(Z)]-	$C_{13}H_{26}$	–	4.33	5.925
	9-Eicosene, (E)-	$C_{20}H_{40}$	–	2.44	10.808
	Heptacos-1-ene	$C_{27}H_{54}$	415	1.00	21.175
	1-Nonadecene	$C_{19}H_{38}$	181	1.02	21.781
Alcohols	n-Tridecan-1-ol	$C_{13}H_{28}O$	155	0.86	6.900
	(2,4,6-Trimethylcyclohexyl)methanol	$C_{10}H_{20}O$	–	0.77	7.450
	1-Decanol, 2-hexyl-	$C_{16}H_{34}O$	304	3.27	21.458
	1-Decanol, 2-hexyl-	$C_{16}H_{34}O$	304	2.95	17.001
	1-Decanol, 2-hexyl-	$C_{16}H_{34}O$	304	1.11	17.228
	1-Decanol, 2-hexyl-	$C_{16}H_{34}O$	304	1.84	17.636
	11-Methyldodecanol	$C_{13}H_{28}O$	261	4.44	11.550
	11-Methyldodecanol	$C_{13}H_{28}O$	261	8.72	11.767
	1-Heptanol, 2,4-diethyl-	$C_{11}H_{24}O$	223	1.01	12.483
	1-Decanol, 2-hexyl-	$C_{16}H_{34}O$	304	1.66	21.925
	10-Dodecen-1-ol, 7,11-dimethyl-	$C_{14}H_{28}O$	–	1.77	22.092
Esters	Butyric acid, 2-phenyl-, dec-2-yl ester	$C_{20}H_{32}O_2$	–	1.61	10.500
	Hexatriacontyl trifluoroacetate	$C_{38}H_{73}F_3O_2$	867	3.70	21.042
	Nonadecyl pentafluoropropionate	$C_{22}H_{39}F_5O_2$	496	0.81	21.567
	Triacontyl heptafluorobutyrate	$C_{34}H_{61}F_7O_2$	–	1.63	23.858
	Octatriacontyl pentafluoropropionate	$C_{41}H_{77}F_5O_2$	641	1.52	24.158
	Ethyl 14-methylhexadecanoate	$C_{19}H_{38}O_2$	–	1.02	24.275
Organosilicons	Cyclononasiloxane, octadecamethyl-	$C_{18}H_{54}O_9Si_9$	416	1.93	27.488
	Cyclodecasiloxane, eicosamethyl-	$C_{20}H_{60}O_{10}Si_{10}$	452	1.52	29.330
	Cyclodecasiloxane, eicosamethyl-	$C_{20}H_{60}O_{10}Si_{10}$	452	1.40	31.194
	Tetracosamethyl-cyclododecasiloxane	$C_{24}H_{72}O_{12}Si_{12}$	518	1.46	33.140
	Cyclononasiloxane, octadecamethyl-	$C_{18}H_{54}O_9Si_9$	416	0.74	22.272
Cyclic hydrocarbons	Cyclohexane, 1,2,3,5-tetraisopropyl-	$C_{18}H_{36}$	–	0.74	23.633
	Cyclohexane, 1,2,3,5-tetraisopropyl-	$C_{18}H_{36}$	–	1.11	24.350
	Cyclohexane, 1,2,3,5-tetraisopropyl-	$C_{18}H_{36}$	–	1.02	24.708
	Cyclohexane, 1,2,3,5-tetraisopropyl-	$C_{18}H_{36}$	–	2.43	27.208
Ether	Hexacosyl nonyl ether	$C_{35}H_{72}O$	–	0.82	25.892
Thiol	tert-Hexadecanethiol	$C_{16}H_{34}S$	329	1.19	26.567

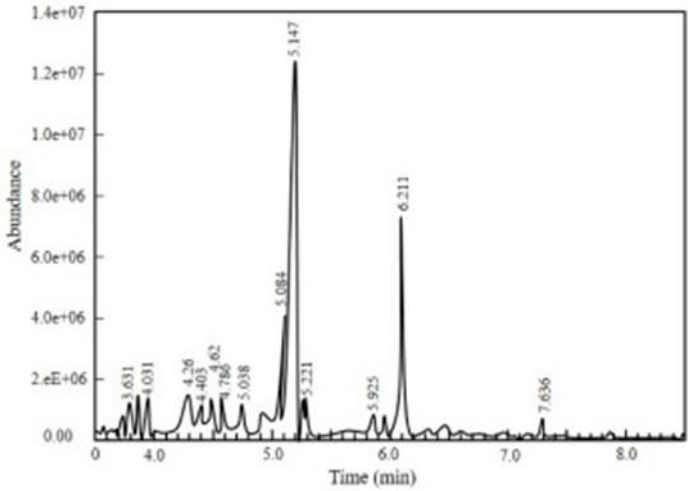

Figure 10. Chromatographic profile of pyrolytic oil from SBW

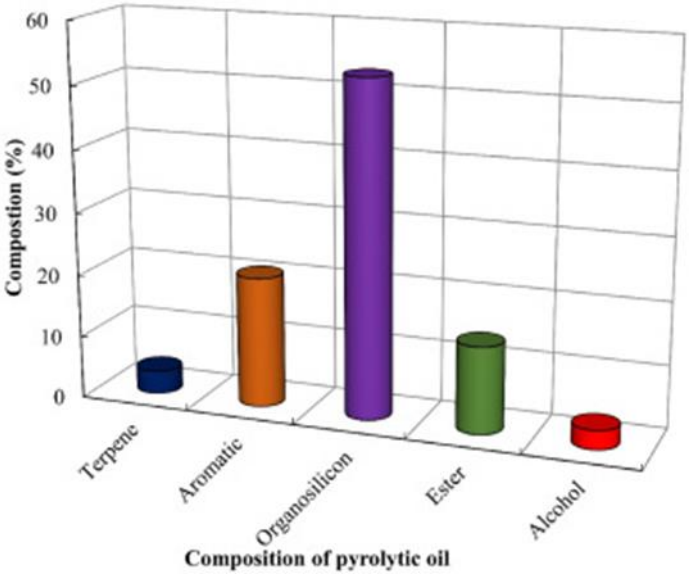

Figure 11. Compositional comparison of pyrolytic oil from SBW

Table 4. Composition of pyrolytic oil from SBW

Compound Class	Compound Name	Molecular Formula	Boiling Point (°C)	Peak Area (%)	Retention Time (min)
Terpene	α-Bisabolol oxide B	$C_{15}H_{26}O_2$	326	3.66	3.419
Aromatic	2-Methyl-5H-dibenz[b,f]azepine	$C_{19}H_{17}N$	359	1.68	3.631
	Oxime-, methoxy-phenyl-	$C_8H_9NO_2$	–	7.29	4.031
	Benzene, 1,4-bis(trimethylsilyl)-	$C_{12}H_{24}Si_2$	194	1.98	5.038
	6-Methyl-2-phenylindole	$C_{15}H_{15}N$	397	8.21	5.084
	Benzoic acid	$C_7H_6O_2$	250	1.62	5.925
Organophosphorus	2-(Dimethylamino)-1,3-dimethyltetrahydro-1,3,2-diazaphosphole 2-oxide	$C_7H_{13}N_2O_2P$	–	1.81	4.260
Ketone	2-Octanone	$C_8H_{16}O$	173	2.32	4.403
Alcohol	2-Ethylhexanol	$C_8H_{18}O$	185	1.61	4.786
	2,5-Hexanediol, 2,5-dimethyl-	$C_8H_{16}O_2$	214	1.39	5.221
Organosilicon	1,1,3,3,5,5-Hexamethyl-cyclohexasiloxane	$C_6H_{18}O_6Si_6$	–	10.64	3.510

	Octamethylcyclotetrasiloxane	$C_8H_{24}O_4Si_4$	175	2.37	4.620
	3,3-Diisopropoxy-1,1,1,5,5,5-hexamethyltrisiloxane	$C_{14}H_{32}O_5Si_3$	–	40.11	5.147
Ester	Perhydro-HTX-2-one, 2-depentyl-, acetate ester	$C_{13}H_{24}O_3$	–	13.81	6.211
Ether	3,4-Dihydroxybenzyl alcohol, tris(trimethylsilyl)-	$C_{17}H_{32}O_3Si_3$	363	1.48	7.636

Characterization of pyrolytic oil by FT-IR

Fourier-transform infrared spectroscopy (FT-IR) provides qualitative and semi-quantitative insight into the chemical families and functional groups present in organic and inorganic materials. The FT-IR tests were conducted at BCSIR, Dhaka. **Figures 12 and 13** depict the spectra of oils obtained at 450 °C from SW and SBW, respectively.

In **Figures 12**, a band at 1781.28 cm^{-1} (C=O stretching) signifies the presence of carboxylic acids. The peak at 2191.64 cm^{-1} corresponds to –C≡C– stretching, indicating alkynes. Alkanes appear at 2958 cm^{-1} through C–H stretching. Signals at 3393.78 cm^{-1} and 3398.6 cm^{-1} denote O–H stretching and hydrogen-bond vibrations characteristic of alcohols. Similar functional groups have been reported in oils from disposable syringe pyrolysis [24, 28]. The spectrum aligns well with the GC-MS results and suggests contributions from polypropylene and polyethylene.

In **Figure 13**, the band at 668.34 cm^{-1} (C–Cl stretching) suggests alkyl halides. Alkenes are identified at 1637.58 cm^{-1} via C=C stretching. Absorptions at 3237.06 cm^{-1}, 3409.21 cm^{-1}, 3412.59 cm^{-1}, 3419.82 cm^{-1}, and 3480.58 cm^{-1} correspond to alcohol and phenolic O–H vibrations, including hydrogen bonding. These findings are consistent with the GC-MS characterization and point to polypropylene and polyethylene origins. **Table 5** lists the characteristic absorption peaks (cm^{-1}) observed in the spectra.

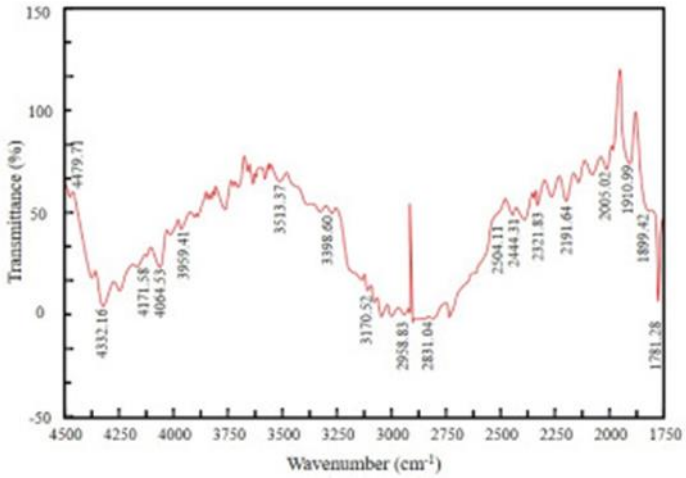

Figure 12. FT-IR profile for oil produced from SW

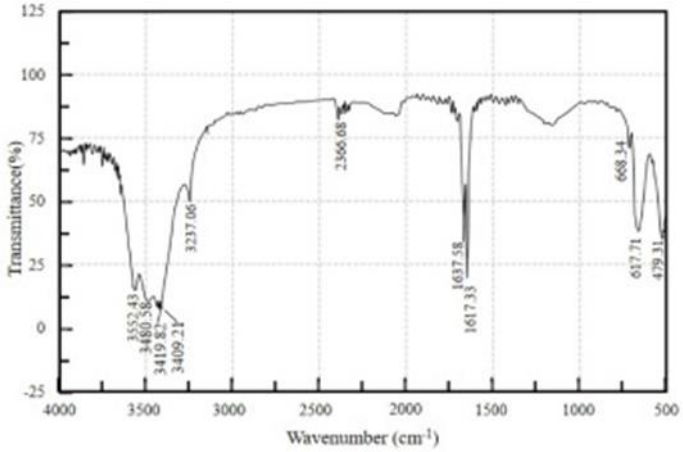

Figure 13. FT-IR profile for oil generated from SBW

Table 5. Identified FT-IR bands and associated functional groups for oils from SW and SBW

Functional Group	Wavenumber (cm^{-1}) – Pyrolytic Oil from SW	Wavenumber (cm^{-1}) – Pyrolytic Oil from SBW	Bond / Vibration	Typical Compound Class
C–Cl	600–800	–	C–Cl stretch	Alkyl halides
C=C	1620–1680	–	C=C stretch	Alkenes
C=O	1670–1820	–	C=O stretch	Carbonyl compounds (ketones, aldehydes, esters, etc.)
–C≡C–	2100–2260	–	C≡C stretch	Alkynes
C–H	2850–3000	–	C–H stretch	Alkanes (and alkyl chains)
O–H (H-bonded)	3200–3600	3200–3600	O–H stretch (broad)	Alcohols, phenols

Comparison of properties of evolved pyrolytic oil with other commercial fuels

The performance-related characteristics of the oils obtained from the two categories of medical plastic waste are important for evaluating their potential usefulness. Since the largest liquid fraction appeared at 450°C, only oils collected at this temperature from SW and SBW were included in the comparison. These property values are listed in **Table 6**.

According to **Table 6**, the densities of the oils from SW and SBW fall close to that of gasoline but remain below diesel values. Their kinematic viscosities are a little higher than those of gasoline, while still comparable to diesel. The pour, boiling, and cloud points nearly match the values typical for gasoline and diesel. The GCV values determined for the SW- and SBW-derived oils in this study also align with the energy content of those commercial fuels. With adequate upgrading, oils from these two waste streams could be utilized in various industrial settings.

Table 6. Comparison of properties for pyrolytic liquids from SW and SBW with gasoline and diesel

Physical Property	Pyrolytic Oil from Syringe Waste (SW)	Pyrolytic Oil from Saline Bottle Waste (SBW)	Gasoline [28, 54]	Diesel [28, 54]
Density at 15 °C (kg/m^3)	758	726	720	840
Kinematic viscosity at 40 °C (cSt)	4.75	3.19	0.6	2–5.5
Pour point (°C)	−12	−16	−40	−40 to −1
Initial boiling point (°C)	95	86	27–225	172–355
Cloud point (°C)	−2	−5	–	−9
Gross calorific value (MJ/kg)	41.519	43.578	42–46	42–45

GCV of syringe waste and saline bottle waste in different states

Measurements of GCV were performed for SW and SBW in their original form, as pyrolytic oils, and as chars. The outcomes are compiled in **Table 7**.

From **Table 7**, the calorific values of the pyrolysis oil and char produced from SW show a slight rise compared with raw SW. For SBW, the pyrolysis oil exhibits a somewhat higher GCV than untreated SBW, whereas the raw and charred SBW display nearly equal heating values. The GCV for raw SW is lower than that of SBW, which is consistent with the fixed-carbon percentages noted in **Table 2**, although both materials fall within the range commonly seen for petrol or diesel oils [28].

Table 7. GCV of SW and SBW in multiple conditions

Waste Material	Gross Calorific Value of Raw Waste (MJ/kg)	Gross Calorific Value of Pyrolytic Oil (MJ/kg)	Gross Calorific Value of Pyrolytic Char (MJ/kg)
Syringe waste (SW)	41.06	41.519	42.737
Saline bottle waste (SBW)	43.31	43.578	43.319

Conclusion

A fixed-bed unit was built to thermochemically convert SW and SBW into liquid, gaseous, and solid fractions. The highest oil and char outputs for SW were 53.2% at 450°C and 73.1% at 50°C. Likewise, SBW yielded 54.9% oil at 450°C and 72.1% char at 50°C. This conversion pathway can help mitigate disposal issues related to waste syringes and saline bottles while supplying alternative fuel sources and chemical feedstocks.
Further work should explore how factors such as heating rate, feed particle dimensions, residence times, and reactor variability influence final yields. GC-MS examination of oils from SW and SBW confirmed numerous industrially relevant molecules. FT-IR profiles supported these findings by revealing a substantial proportion of hydrocarbon-type functionalities. Using catalysts is strongly recommended to upgrade product quality. The solid char obtained from both waste types could be densified with binders for use as fuel or transformed into activated carbon. Pyrolysis of SW and SBW also reduces the environmental risks tied to uncontrolled disposal, and the study emphasizes the need for better handling of plastic-based medical residues.

Acknowledgments: This experiment was conducted in the Heat Engine Laboratory of the Department of Mechanical Engineering, Khulna University of Engineering & Technology (KUET), Khulna-9203, Bangladesh. The authors would like to acknowledge the Vice-Chancellor of Khulna University of Engineering & Technology (KUET) for the financial support during the project work to conduct this experiment. The technical support from the technical staff of CARS, DU, and BCSIR for chemical analysis is also gratefully acknowledged.

Conflict of Interest: None

Financial Support: None

Ethics Statement: None

References

1. A.K. Panda, R.K. Singh, D.K. Mishra, Thermolysis of waste plastics to liquid fuel: a suitable method for plastic waste management and manufacture of value- added products-A world perspective, Journal of Renewable and Sustainable Energy Reviews 14 (1) (2010) 233–248, https://doi.org/10.1016/j. rser.2009.07.005.
2. Y.W. Cheng, F.C. Sung, Y. Yang, Y.H. Lo, Y.T. Chung, K.C. Li, Medical waste production at hospitals and associated factors, Journal of Waste Management 29 (1) (2009) 440–444, https://doi.org/10.1016/j.wasman.2008.01.014.
3. M.F. Hassan, Z. Shareefdeen, Recent developments in sustainable management of healthcare waste and treatment technologies, Journal of Sustainable Development of Energy, Water and Environment Systems 10 (2) (2022) 1–21, https://doi.org/10.13044/j.sdewes.d9.0384.
4. M. Sartaj, R. Arabgol, Assessment of healthcare waste management practices and associated problems in Isfahan Province (Iran), J. Mater. Cycles Waste Manag. 17 (2015) 99–106, https://doi.org/10.1007/s10163-014-0230-5.
5. L.F. Diaz, L.L. Eggerth, S.H. Enkhtsetseg, G.M. Savage, Characteristics of healthcare wastes, Waste management 28 (7) (2008) 1219–1226, https://doi.org/ 10.1016/j.wasman.2007.04.010.
6. D.P. Komilis, Issues on medical waste management research, Journal of Waste Management 100 (48) (2016) 1–2, https://doi.org/10.1016/j. wasman.2015.12.020.
7. B. Mbongwe, B.T. Mmereki, A. Magashula, Healthcare waste management: current practices in selected healthcare facilities, Botswana, Journal of Waste Management 28 (1) (2008) 226–233, https://doi.org/10.1016/j.wasman.2006.12.019.
8. U. Som, F. Rahman, S. Hossain, Recovery of pyrolytic oil from thermal pyrolysis of medical waste, Journal of Engineering Sciences 5 (2) (2018) H5–H8, https:// doi.org/10.21272/jes.2018.5(2).h2.
9. A. Lopez, I. De Marco, B.M. Caballero, M.F. Laresgoiti, A. Adrados, Influence of time and temperature on pyrolysis of plastic wastes in a semi-batch reactor, J. Chem. Eng. 173 (1) (2011) 62–71, https://doi.org/10.1016/j.cej.2011.07.037.

10. L. Dai, N. Zhou, Y. Lv, Y. Cheng, Y. Wang, Y. Liu, K. Cobb, P. Chen, H. Lei, R. Ruan, Pyrolysis technology for plastic waste recycling: a state-of-the-art review, Prog. Energy Combust. Sci. 93 (2022) 101021, https://doi.org/10.1016/j.pecs.2022.101021.
11. S. Budati, A.P. Reddy, N.R. Prasad, N. Shaik, Management of COVID-19 medical waste based on pyrolysis-swot analysis, Int J Acad Med Pharm 6 (1) (2024) 647–655, https://doi.org/10.47009/jamp.2024.6.1.129.
12. N.C˘. Kantov´a, R. Cibula, A. Szlek, A. C˘aja, R. Nosek, P. Belany, The energy assessment of COVID-19 medical waste as a potential fuel, Energy Rep. 9 (2023) 4995–5003, https://doi.org/10.1016/j.egyr.2023.04.018.
13. R. Choudhary, A. Mukhija, S. Sharma, R. Choudhary, A. Chand, A.K. Dewangan, G.K. Gaurav, J.J. Kleme˘s, Energy-saving COVID–19 biomedical plastic waste treatment using the thermal-Catalytic pyrolysis, Energy 264 (2023) 126096, https://doi.org/10.1016/j.energy.2022.126096.
14. S. Ramalingam, R. Thamizhvel, S. Sudagar, R. Silambarasan, Production of third generation bio-fuel through thermal cracking process by utilizing Covid-19 plastic wastes, Mater. Today Proc. 72 (2023) 1618–1623, https://doi.org/10.1016/j.matpr.2022.09.430.
15. S. Dharmaraj, V. Ashokkumar, R. Pandiyan, H.S.H. Munawaroh, K.W. Chew, W.H. Chen, C. Ngamcharussrivichai, Pyrolysis: an effective technique for degradation of COVID-19 medical wastes, Chemosphere 275 (2021) 130092, https://doi.org/10.1016/j.chemosphere.2021.130092.
16. C. Chen, J. Chen, R. Fang, F. Ye, Z. Yang, Z. Wang, F. Shi, W. Tan, What medical waste management system may cope with COVID-19 pandemic: lessons from Wuhan, Resour. Conserv. Recycl. 170 (2021) 105600, https://doi.org/10.1016/j.resconrec.2021.105600.
17. G. Su, H.C. Ong, S. Ibrahim, I.R. Fattah, M. Mofijur, C.T. Chong, Valorisation of medical waste through pyrolysis for a cleaner environment: progress and challenges, Environmental Pollution 279 (2021) 116934, https://doi.org/10.1016/j.envpol.2021.116934.
18. J.S. Jeba, M.M. Rahman, Medical waste management in Khulna city corporation, Bangladesh, Natl. Geogr. J. India 66 (4) (2022) 306–319, https://doi.org/ 10.48008/ngji.1750.
19. M.S. Rahman, C. Moumita, K. Rikta, Medical waste management system: an alarming threat (A case study on jessore municipality, Bangladesh), Journal of Environmental Science and Natural Resources 6 (2) (2013) 181–189, https://doi.org/10.3329/jesnr.v6i2.22115.
20. M.Z. Alam, M.S. Islam, M.R. Islam, Medical waste management: a case study on Rajshahi city corporation in Bangladesh, Journal of Environmental Science and Natural Resources 6 (1) (2013) 173–178, https://doi.org/10.3329/jesnr.v6i1.22062.
21. F. Ullah, G. Ji, L. Zhang, M. Irfan, Z. Fu, Z. Manzoor, A. Li, Assessing pyrolysis performance and product evolution of various medical wastes based on model-free and TG-FTIR-MS methods, Chem. Eng. J. 473 (2023) 145300, https://doi.org/10.1016/j.cej.2023.145300.
22. W. Xu, J. Liu, Z. Ding, J. Fu, F. Evrendilek, W. Xie, Y. He, Dynamic pyrolytic reaction mechanisms, pathways, and products of medical masks and infusion tubes, Sci. Total Environ. 842 (2022) 156710, https://doi.org/10.1016/j.scitotenv.2022.156710.
23. Z. Ding, H. Chen, J. Liu, H. Cai, F. Evrendilek, M. Buyukada, Pyrolysis dynamics of two medical plastic wastes: drivers, behaviors, evolved gases, reaction mechanisms, and pathways, J. Hazard Mater. 402 (2021) 123472, https://doi.org/10.1016/j.jhazmat.2020.123472.
24. C. Vasile, M. Brebu, H. Darie, R.D. Deanin, V. Dorneanu, D.M. Pantea, O.G. Ciochina, Chemicals and energy from medical polymer wastes I. Pyrolysis of disposable syringes, Int. J. Polym. Mater. 38 (3–4) (1997) 219–247, https://doi.org/10.1080/00914039708041020.
25. N. Deng, Y.F. Zhang, Y. Wang, Thermogravimetric analysis and kinetic study on pyrolysis of representative medical waste composition, Journal of Waste Management 28 (9) (2008) 1572–1580, https://doi.org/10.1016/j.wasman.2007.05.024.
26. H.M. Zhu, J.H. Yan, X.G. Jiang, Y.E. Lai, K.F. Cen, Study on pyrolysis of typical medical waste materials by using TG-FT-IR analysis, J. Hazard Mater. 153 (1–2) (2008) 670–676, https://doi.org/10.1016/j.jhazmat.2007.09.011.
27. M. Bernardo, N. Lapa, M. Gonçalves, B. Mendes, F. Pinto, I. Fonseca, H. Lopes, Physico-chemical properties of chars obtained in the co-pyrolysis of waste mixtures, J. Hazard Mater. 219 (2012) 196–202, https://doi.org/10.1016/j.jhazmat.2012.03.077.

28. A. Dash, S. Kumar, R.K. Singh, Thermolysis of medical waste (Waste Syringe) to liquid fuel using semi-batch reactor, Journal of Waste and Biomass Valorization 6 (4) (2015) 507–514, https://doi.org/10.1007/s12649-015-9382-3.
29. I. Ahmad, M.I. Khan, H. Khan, M. Ishaq, R. Tariq, K. Gul, W. Ahmad, Pyrolysis study of polypropylene and polyethylene into premium oil products, Int. J. Green Energy 12 (7) (2015) 663–671, https://doi.org/10.1080/15435075.2014.880146.
30. H. Pramanik, P. Gaurh, Production and characterization of pyrolysis oil using waste polyethylene in a semi-batch reactor, Indian J. Chem. Technol. 25 (4) (2019) 336–344, https://doi.org/10.56042/ijct.v25i4.15134.
31. P.T. Williams, S. Besler, The influence of temperature and heating rate on the slow pyrolysis of biomass, Journal of Renewable energy 7 (3) (1996) 233–250, https://doi.org/10.1016/0960-1481(96)00006-7.
32. S.H. Jung, M.H. Cho, B.S. Kang, J.S. Kim, Pyrolysis of a fraction of waste polypropylene and polyethylene for the recovery of BTX aromatics using a fluidized bed reactor, Journal of Fuel Processing Technology 91 (3) (2010) 277–284, https://doi.org/10.1016/j.fuproc.2009.10.009.
33. M.Z.H. Khan, M. Sultana, M.R.A. Al-Mamun, M.R. Hasan, Pyrolytic waste plastic oil and its diesel blend: fuel characterization, Journal of Environmental and Public Health 2016 (2016) 1–6, https://doi.org/10.1155/2016/7869080.
34. A. Lo´pez, I. de Marco, B.M. Caballero, M.F. Laresgoiti, A. Adrados, Pyrolysis of municipal plastic wastes: influence of raw material composition, Journal of Waste Management 30 (4) (2010) 620–627, https://doi.org/10.1016/j.wasman.2009.10.014.
35. A. Adrados, I. De Marco, B.M. Caballero, A. Lo´pez, M.F. Laresgoiti, A. Torres, Pyrolysis of plastic packaging waste: a comparison of plastic residuals from material recovery facilities with simulated plastic waste, Journal of Waste Management 32 (5) (2012) 826–832, https://doi.org/10.1016/j. wasman.2011.06.016.
36. A. Brems, J. Baeyens, C. Vandecasteele, R. Dewil, Polymeric cracking of waste polyethylene terephthalate to chemicals and energy, J. Air Waste Manag. Assoc. 61 (7) (2011) 721–731, https://doi.org/10.3155/1047-3289.61.7.721.
37. A.M. Widiyannita, R.B. Cahyono, A. Budiman, Sutijan, T. Akiyama, Study of pyrolysis of ulin wood residues, in: AIP Conference Proceedings, vol. 1755, AIP Publishing LLC, 2016, July 050004, https://doi.org/10.1063/1.4958487, 1.
38. M.A. Patwary, W.T. O'Hare, G. Street, K.M. Elahi, S.S. Hossain, M.H. Sarker, Quantitative assessment of medical waste generation in the capital city of Bangladesh, Journal of Waste Management 29 (8) (2009) 2392–2397, https://doi.org/10.1016/j.wasman.2009.03.021.
39. S.R. Basak, A.F. Mita, N.J. Ekra, M.J.B. Alam, A study on hospital waste management of Sylhet city in Bangladesh, International Journal of Engineering Applied Sciences and Technology 4 (2019) 36–40, https://doi.org/10.33564/ijeast.2019.v04i05.006.
40. A.D. Patil, A.V. Shekdar, Healthcare waste management in India, J. Environ. Manag. 63 (2) (2001) 211–220, https://doi.org/10.1006/jema.2001.0453.
41. E.S. Windfeld, M.S.L. Brooks, Medical waste management–A review, J. Environ. Manag. 163 (2015) 98–108, https://doi.org/10.1016/j.jenvman.2015.08.013.
42. O.L. Rabeie, M.B. Miranzadeh, S.H. Fallah, S. Dehqan, Z. Moulana, A. Amouei, A.A. Mohammadi, H.A. Asgharnia, M. Babaie, Determination of hospital waste composition and management in Amol city, Iran, Journal of Health Scope 1 (3) (2012) 127–131, https://doi.org/10.17795/jhealthscope-6305.
43. A.P. Ananth, V. Prashanthini, C. Visvanathan, Healthcare waste management in Asia, Journal of Waste Management 30 (1) (2010) 154–161, https://doi.org/ 10.1016/j.wasman.2009.07.018.
44. S. Tantanee, S. Hantrakul, Municipal waste management challenge of urbanization: lesson learned from phitsanulok, Thailand, Geogr. Tech. 14 (2019), https:// doi.org/10.21163/gt_2019.141.17.
45. E. Bazrafshan, F. Kord Mostafapoor, Survey of medical waste characterization and management in Iran: a case study of Sistan and Baluchestan Province, Journal of Waste Management & Research 29 (4) (2011) 442–450, https://doi.org/10.1177/0734242X10374901.
46. S. Phengxay, J. Okumura, M. Miyoshi, K. Sakisaka, C. Kuroiwa, M. Phengxay, Healthcare waste management in Lao PDR: a case study, Journal of Waste Management & Research 23 (6) (2005) 571–581, https://doi.org/10.1177/0734242X05059802.

47. Z. Yong, X. Gang, W. Guanxing, Z. Tao, J. Dawei, Medical waste management in China: a case study of Nanjing, Journal of Waste management 29 (4) (2009) 1376–1382, https://doi.org/10.1016/j.wasman.2008.10.023.
48. R. Gai, C. Kuroiwa, L. Xu, X. Wang, Y. Zhang, H. Li, C. Zhou, J. He, W. Tang, C. Kuroiwa, W. Tang, Hospital medical waste management in Shandong Province, China, Journal of Waste management & research 27 (4) (2009) 336–342, https://doi.org/10.1177/0734242X09104384.
49. M.S. Hossain, A. Santhanam, N.N. Norulaini, A.M. Omar, Clinical solid waste management practices and its impact on human health and environment-A review, Journal of Waste Management 31 (4) (2011) 754–766, https://doi.org/10.1016/j.wasman.2010.11.008.
50. H.H. Eker, M.S. Bilgili, Statistical analysis of waste generation in healthcare services: a case study, Journal of Waste Management & Research 29 (8) (2011) 791–796, https://doi.org/10.1177/0734242X10396755.
51. R.K. Singh, B. Ruj, A.K. Sadhukhan, P. Gupta, Thermal degradation of waste plastics under non-sweeping atmosphere: Part 1: effect of temperature, product optimization, and degradation mechanism, J. Environ. Manag. 239 (2019) 395–406, https://doi.org/10.1016/j.jenvman.2019.03.067.
52. M.S. Hossain, A. Abedeen, M.R. Karim, M. Moniruzzaman, M.J. Hosen, Catalytic pyrolysis of waste tires: the influence of ZSM-catalyst/tire ratio on product, Iran. J. Energy Environ. 8 (3) (2017) 189–193, https://doi.org/10.5829/ijee.2017.08.03.02.
53. S. Fang, L. Jiang, P. Li, J. Bai, C. Chang, Study on pyrolysis product characteristics of medical waste and fractional condensation of the pyrolysis oil, Energy 195 (2020) 116969, https://doi.org/10.1016/j.energy.2020.116969.
54. F. Ullah, L. Zhang, G. Ji, M. Irfan, D. Ma, A. Li, Experimental analysis on product distribution and characterization of medical waste pyrolysis with a focus on liquid yield quantity and quality, Sci. Total Environ. 829 (2022) 154692, https://doi.org/10.1016/j.scitotenv.2022.154692.